

# A MODEL FOR CURING IN RUBBER MOLDING USING THE FINITE ELEMENT TOOLBOX ALBERTA

Daniel Koester  
LAM1 - Universität Augsburg  
Universitätsstrasse 14  
D-86159 Augsburg, Germany  
koester@math.uni-augsburg.de

Paulo Porta  
R&D Unit – DARMEX S.A.C.I.F.I  
Luis María Drago 1555  
B1852LGS, Burzaco, Argentina  
pporta@darmex-int.com

## KEYWORDS

Software and tools, finite elements, ALBERTA toolbox, industrial applications.

## ABSTRACT

A nonlinear, dimensionless model for the curing *in situ* of rubber elements is presented and analyzed. This results in a coupled nonlinear differential equations system. To solve it, we pose a semi-implicit linearized FEM model and implement it using the finite element toolbox ALBERTA. We test the implementation in the two dimensional case of a rubber bladder, giving numerical results and an analysis of the performance.

## INTRODUCTION

A large number of polymer products are formed into their final shape by polymerization *in situ*. Examples include (see e.g. Mark *et al.* 2005 for more details) processes like monomer casting, potting or encapsulation, bonding with structural adhesives, reinforced plastic lamination, and thermoset and rubber molding operations.

Of particular interest in this paper is the case of rubber bladders molding. This kind of element is used in several manufacturing processes as for example in tire manufacturing. The bladder fabrication process may be described as composed of three steps: *i*) the mold filling, *ii*) the *in situ* curing and *iii*) post cure, when the element is cooled down to room temperature. Clearly, from the point of view of industrial applications, determination of optimal *in situ* curing time is the single most important objective (In-Su Han *et al.* 1999).

In this sense, simulation of a rubber curing process can considerably influence the costs and quality of the process. There are several articles, reporting previous work in this field (see, e.g. Broyer and Macoskos. 1976, Juma and Bafnec 2004, Andre and Wriggers 2005, Ghoreishy and Naderi 2005). A balance of internal heat generation and heat transfer through the mold walls controls polymer reaction molding processes. In what follows, a nonlinear model is constructed and a solution scheme is proposed, and an implementation based on the ALBERTA finite element toolbox is presented, together with numerical results.

## THE MODEL

### Background

The model is constructed from the Reynolds transport theorem, which describes the total change in time of a quantity in terms of the local and convective variations of that quantity. Let us consider a fixed and arbitrary control volume  $\Omega$ . Let  $N$  be an extensive quantity and  $\eta$  its corresponding intensive expression. Then the application of the theorem results in

$$\int_{\Omega} \frac{\partial}{\partial t} \rho \eta d^3x + \oint_{\partial\Omega} \rho \eta \vec{V} da = \int_{\Omega} \text{div}(\kappa \text{grad} \eta) d^3x + \int_{\Omega} S_N d^3x \quad (1)$$

where  $\vec{V}$  is the convection velocity,  $S_N$  is a source for the quantity  $N$ ,  $\rho$  the density and  $da$  the area element over the closed surface  $\partial\Omega$ . This equation will be applied to the cases in which  $N$  is alternatively heat and mass of reactant, in which cases  $\eta$  is the temperature  $\Theta$ , and concentration  $\chi$ , respectively.

Of the three steps of the curing process described above, the second will be of interest –the *in situ* curing– because it is the one that requires more control. This step initiates once the press is closed and the mold is filled with rubber. At this point the rubber is immobilized and thus there is no transport of heat or mass due to convection. This implies that the second term of the left hand side in Equation (1) vanishes.

In the case of heat, this observation yields

$$\frac{\partial \Theta}{\partial t} = \text{div}(\kappa \text{grad} \eta) + \frac{q'}{\rho c_p}, \quad (2)$$

the transient heat conduction equation, with internal heat source. This source is due to the exothermic curing reaction and may be modeled linearly as

$$q' = H_r R_{\chi} \quad (3)$$

that is, proportional to the reaction enthalpy,  $H_r$ , and to the reaction rate  $R_{\chi}$ .

Rubber being an amorphous material, thermal diffusivity, specific heat and density exhibit very little change when solidifying or in the range of temperatures of the process, so they will be considered constant. Furthermore, the reaction temperature will also be considered constant.

In the case of mass, we have an equation similar to Equation (2), namely

$$\frac{\partial \chi}{\partial t} = \text{div}(D \text{grad } \chi) + R_\chi \quad (4)$$

In normal conditions of process, the compound is sufficiently mixed and homogenized, thus the diffusion mechanism is dominated by the changes due to reaction. Typically, reactants have molecular weights of the order of  $10^2$  and viscosities are of the order of 1 poise or more. Using the Stokes/Einstein equation, the diffusivity is of the order of

$$D = \frac{k_B \Theta}{6\pi r \eta}$$

so that, for the usual temperatures of process,  $D < 10^{-9} \text{ cm}^2 / \text{sec}$ . Typically,  $O(R_\chi) \approx 10^{-4} \frac{\text{mol}}{\text{lsec}}$ : to compare the relative influence of the two terms in the right hand side of Equation (4), observe that for a reactant reference concentration of  $0.2 \frac{\text{mol}}{\text{l}}$  and a characteristic length of  $10 \text{ mm}$ ,

$$D|\Delta \chi|_{\max} \approx 10^{-9} \frac{\text{mol}}{\text{lsec}} \ll O(R_\chi).$$

With this argument the diffusion process is neglected when compared with the reaction mechanism, and the reaction equation adopts the form

$$\frac{d\chi}{dt} = R_\chi \quad (5)$$

The kinetic of the reaction may be modeled in several ways. In this work, following Broyer and Macoskos, 1976, and In-Su Han *et al.* 1999, a reaction of order  $\gamma$  is adopted

$$R_\chi = -K_\chi^{(\gamma)} \chi^\gamma, \quad (6)$$

where the minus indicates the decay in the reactant amount and  $K_\chi^{(\gamma)}$  responds to an Arrhenius equation

$$K_\chi^{(\gamma)} = K_{\chi_0}^{(\gamma)} \exp\left(-\frac{E_\chi}{R\Theta}\right) \quad (7)$$

With this expressions, Equations (5), (6) and (7) yield

$$-\frac{d\chi}{dt} = K_{\chi_0}^{(\gamma)} \exp\left(\frac{E_\chi}{R\Theta}\right) \chi^\gamma. \quad (8)$$

Collecting Equations (2), (3), (6) and (7) the heat equation may be expressed in terms of concentration of reactant and temperature. The resulting equation, together with Equation (8) define our mathematical model, namely

$$\begin{cases} \frac{\partial \Theta}{\partial t} = \kappa \Delta \Theta + \frac{H_r}{\rho c_p} K_{\chi_0}^{(\gamma)} \exp\left(-\frac{E_\chi}{R\Theta}\right) \chi^\gamma \\ -\frac{d\chi}{dt} = K_{\chi_0}^{(\gamma)} \exp\left(-\frac{E_\chi}{R\Theta}\right) \chi^\gamma \end{cases} \quad (9)$$

### The dimensionless equations

Let  $\ell$  represent the characteristic length of the domain,  $\chi_0$  be the reference concentration of reactant and  $\Theta_0$  the reference temperature. Define the following dimensionless variables

$$\tau = \frac{\kappa}{\ell^2} t, \quad \zeta_i = \frac{x_i}{\ell}, \quad X = \frac{\chi}{\chi_0}, \quad \vartheta = \frac{\Theta}{\Theta_0}. \quad (10)$$

Replacing these variables in Equations (9), three dimensionless groups arise

$$\begin{aligned} \Theta_{ad} &= \frac{H_r \chi_0}{\rho c_p \Theta_0} \\ B &= \frac{E_\chi}{R\Theta_0} \\ \tilde{K}_\chi^{(\gamma)} &= \frac{\ell^2 \chi_0^{\gamma-1} K_{\chi_0}^{(\gamma)} e^{-B}}{\kappa} \end{aligned} \quad (11)$$

the adiabatic temperature, the dimensionless activation energy and the dimensionless reaction rate, respectively. The dimensionless version of the governing system results in

$$\begin{cases} \frac{\partial \vartheta}{\partial \tau} = \Delta \vartheta + \Theta_{ad} \tilde{K}_\chi^{(\gamma)} \exp\left(B\left(1 - \frac{1}{\vartheta}\right)\right) X^\gamma \\ -\frac{dX}{d\tau} = \tilde{K}_\chi^{(\gamma)} \exp\left(B\left(1 - \frac{1}{\vartheta}\right)\right) X^\gamma \end{cases} \quad (12)$$

This system of differential equations must be supplemented with initial and boundary conditions, namely

$$X = X_0 \quad \vartheta = \vartheta_0 \quad \forall \bar{c} \in \Omega, t = 0$$

$$\vartheta = \vartheta_D \text{ on } \Gamma^D, \quad \bar{n} \cdot \kappa \cdot \text{grad} \vartheta = q'_N \text{ on } \Gamma^N$$

where  $\Gamma^D$  is the part of the boundary over which Dirichlet boundary conditions are prescribed and  $\Gamma^N$  the corresponding part over which Neumann boundary conditions are imposed, such that  $\partial\Omega = \Gamma^D \cup \Gamma^N$ .

## THE IMPLEMENTATION

### The algorithm

System (12) consists of a coupled ODE initial value problem/PDE initial–boundary value problem. The following algorithm is proposed to solve it

ALGORITHM 1: Given  $(X_0, \vartheta_0, \vartheta_D, q'_N)$ , for  $n = 1, 2, \dots$

1. Solve for  $X$  in every point of the domain at instant  $\tau_n > \tau_{n-1}$  the ordinary differential reaction equation initial value problem with an explicit scheme.
2. With  $X(\tau_n)$ , solve for  $\vartheta$  in every point of the domain at instant  $\tau_n > \tau_{n-1}$  the PDE initial–boundary value problem for heat equation.

### Numerical scheme for the reaction equation

To solve the initial value ODE problem, as proposed in Algorithm 1, an explicit scheme is built for the reaction equation. In particular, fourth order Runge-Kutta is used in the form

$$X_n = X_{n-1} + \frac{\Delta t}{6} (k_1 + 2k_2 + 2k_3 + k_4)$$

where

$$\begin{aligned} k_1 &= -\tilde{K}_x^{(\gamma)} \exp\left(B\left(1 - \frac{1}{\vartheta_{n-1}}\right)\right) X_{n-1}^\gamma \\ k_2 &= -\tilde{K}_x^{(\gamma)} \exp\left(B\left(1 - \frac{1}{\vartheta_{n-1}}\right)\right) \left(X_{n-1} + \frac{\Delta t}{2} k_1\right)^\gamma \\ k_3 &= -\tilde{K}_x^{(\gamma)} \exp\left(B\left(1 - \frac{1}{\vartheta_{n-1}}\right)\right) \left(X_{n-1} + \frac{\Delta t}{2} k_2\right)^\gamma \\ k_4 &= -\tilde{K}_x^{(\gamma)} \exp\left(B\left(1 - \frac{1}{\vartheta_{n-1}}\right)\right) \left(X_{n-1} + \Delta t k_3\right)^\gamma \end{aligned}$$

### The weak and finite element formulations for the heat equation

As before, let  $\Gamma^D$  be the part of the boundary over which Dirichlet boundary conditions are prescribed and  $\Gamma^N$  the corresponding part over which Neumann boundary conditions are imposed, such that  $\partial\Omega = \Gamma^D \cup \Gamma^N$ . Moreover, define  $H = H^1(\Omega)$  and  $H_0 = \{v \in H : v = 0 \in \Gamma^D\}$ . Let  $\vartheta_n$  indicate the dimensionless temperature at time  $t_n$ , such that  $\theta_n \in H$ . The following weak problem is formulated

**PROBLEM 1:** Given  $X_{n+1} \in L^2$ , find  $\vartheta_{n+1}$ , with  $\vartheta_{n+1}|_{\Gamma^D} = \vartheta_D$ , for  $\psi \in H_0$  such that

$$\begin{aligned} \frac{1}{\Delta t} \int_{\Omega} \psi \vartheta_{n+1} + \int_{\Omega} \text{grad} \psi \cdot \text{grad} \vartheta_{n+1} &= \int_{\Gamma^D} \psi q'_N + \\ &+ \int_{\Omega} \psi \Theta_{ad} \tilde{K}_x^{(\gamma)} \exp\left[B\left(1 - \frac{1}{\vartheta_n}\right)\right] X_{n+1}^\gamma + \frac{1}{\Delta t} \int_{\Omega} \psi \vartheta_n \end{aligned}$$

The finite element approximation of Problem 1 is constructed as follow: let  $\Omega_h$  be a simplicial triangulation of the domain, defining elements  $E$ . Define  $H_h \subset H$ , and finite dimensional subspace

$$H_{0h} = \{v_h \in H_h : v_h = 0 \text{ on } \Gamma^D\}.$$

**PROBLEM 2:** Given  $X_{h,n+1}$  an approximation of  $X_{n+1}$ ,  $q'_{Nh}$  an approximation for  $q'_N$  and  $\vartheta_{h,n}$ , for  $\psi_h \in H_{0h}$ , find  $\vartheta_{h,n+1}$ , with  $\vartheta_{h,n+1}|_{\Gamma^D} = \vartheta_D$  such that

$$\begin{aligned} \frac{1}{\Delta t} \int_{\Omega} \psi_h \vartheta_{h,n+1} + \int_{\Omega} \text{grad} \psi_h \cdot \text{grad} \vartheta_{h,n+1} &= \int_{\Gamma^D} \psi_h q'_{Nh} + \\ &+ \int_{\Omega} \psi_h \Theta_{ad} \tilde{K}_x^{(\gamma)} \exp\left[B\left(1 - \frac{1}{\vartheta_{h,n}}\right)\right] X_{h,n+1}^\gamma + \frac{1}{\Delta t} \int_{\Omega} \psi_h \vartheta_{h,n} \end{aligned}$$

### The toolbox ALBERTA

Finite element methods calculate approximations to the exact solution of a weak problem in some finite dimensional function space. This space is built from local function spaces, usually polynomials of lower order, on elements of a partitioning of the domain (the mesh). An adaptive method adjusts this mesh (or the local function space or both) to the solution of the problem, based on information from *a posteriori* error estimators.

Starting point for the design of ALBERTA data structures is the abstract concept of a finite element space defined as a triple consisting of *i*) a collection of mesh elements, *ii*) a set of local basis functions on a single element and *iii*) a connection of local and global basis functions giving the global degrees of freedom (Schmidt and Siebert 2005). This directly leads to the definition of three main group of data structures *i*) data structures for geometric information, *ii*) data structure for finite element information and *iii*) data structure for algebraic information. Using these data structures, ALBERTA provides the whole abstract framework like finite element spaces and adaptive strategies, together with the hierarchical meshes, routines for mesh adaptation, and the complete administration of finite

element spaces and the corresponding degrees of freedom during mesh modifications.

A specific problem can be implemented and solved within the ALBERTA framework just providing some problem dependent routines for the evaluation of the (in our case, linearized) differential operator, data, nonlinear solver and error estimators.

## NUMERICAL EXAMPLES

### A one-dimensional test case

In order to validate the model, we have simulated a conductivity test that is routinely performed at DARMEX laboratories. This is a variant of the “Standard Practice for Evaluating Thermal Conductivity of Gasket Materials” (see ASTM F433-02). Two flat samples of identical thicknesses with a thermocouple between them are sandwiched between two plates, one of them with a temperature control and instrumented with a thermocouple. This plate is heated and both temperatures –at the plate and between the probes- are recorded. Any recorded temperature variation will be due both to the transported plates’ heat and to the distributed reaction heat source. In the second plate, a heat flux meter was adapted for control purposes.

The process in this device was modeled with the one dimensional heat equation, coupled with the reaction equation. A Dirichlet boundary condition was imposed on the corresponding plate node and a Neumann boundary condition was imposed on the central node, the prescribed value set in accordance to measured heat flux. The same values for the dimensionless parameters were used both in the numerical and laboratory experiments:  $\Theta_{ad} = 2 \times 10^{-3}$ ,  $B = 22.37$ , and

$\tilde{K}_\chi^{(\gamma)} = 8.48$ . Figure 1 depicts the temperature evolution of the central point as calculated and its departure from the measured values. Maximum departure is less than 8% and occurs at the initial stages, most probably due to both inconsistencies in the experimental determination of the initial state and the initial conditions and experimental errors.

### A two-dimensional example with analytic solution

To verify the correctness of our code, we tried the model on the unit square domain. The simulation is

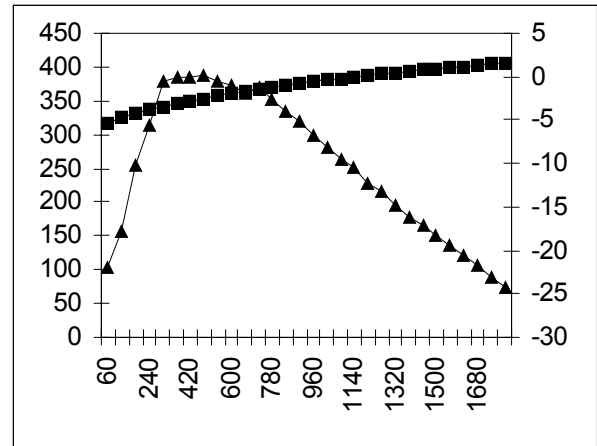


Figure 1: Temperature evolution of the central point of the probe (■, left scale) and departure from the experimental values (▲, right scale)

performed for the same values of the parameters,  $\Theta_{ad} = 2 \times 10^{-3}$ ,  $B = 22.37$ , and  $\tilde{K}_\chi^{(\gamma)} = 8.48$ . The employed regular mesh is depicted in Figure 2.

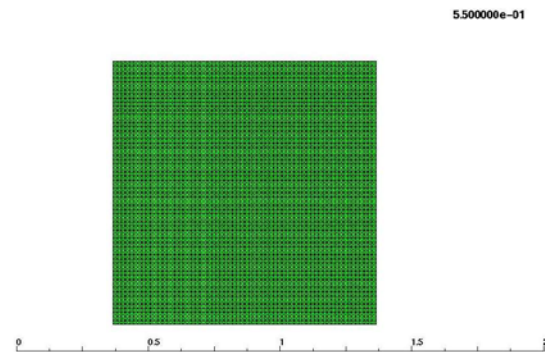


Figure 2: Mesh employed in the square test problem

Figure 3 shows two instants of the simulation: on top the temperature distribution at an early stage of the process is shown. A colder central region is being heated from the outside, due both to the boundary heat and the reaction heat transmission. The bottom part depicts the temperature distribution at a latter stage: an inversion in the distribution of the hot and cold zones is observed: the core of the square is producing heat due to reaction, thus increasing the temperature and heating the outside layers.

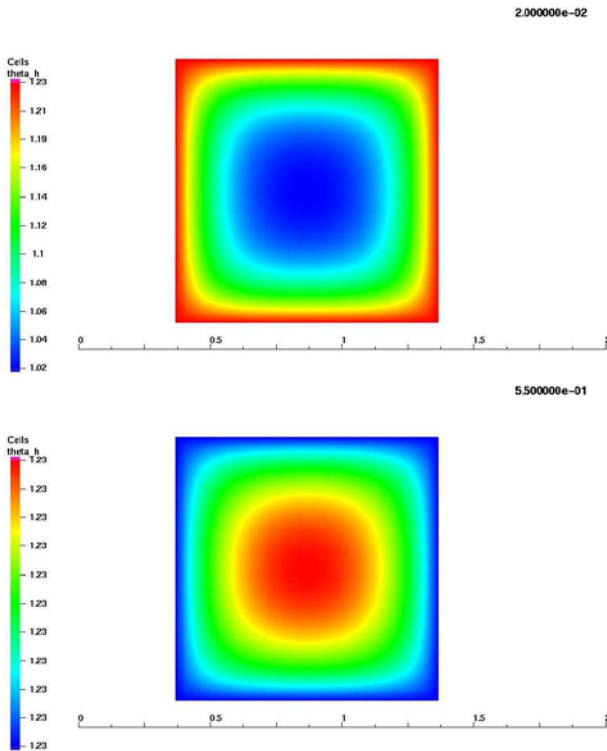


Figure 3: Temperature distribution at two different instants of the process. An inversion in the hot and cold zones may be observed.

### Application to the cure of a rubber bladder

The algorithm was also implemented for the case of a rubber bladder similar to those employed in the tire manufacturing industry. A detail of the mesh used to approximate the geometry is shown in Figure 4.

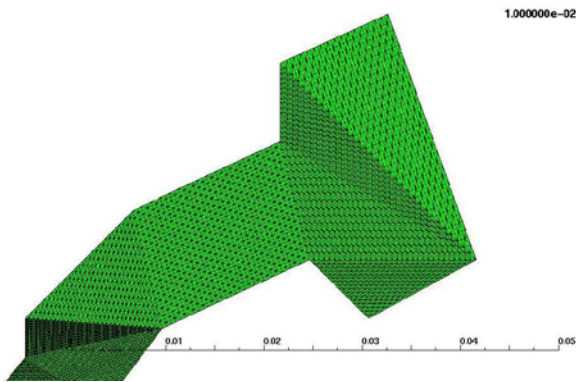


Figure 4: Detail of the mesh employed in the simulation of the bladder curing process.

Figure 5 shows again, the temperature distribution for two instants of the curing process, while Figure 6 shows the concentration of reactant for the latter. With respect to the temperature distribution, the same inversion phenomena is observed; on the other hand, there is no inversion in the reactant's concentration distribution along the simulation, in total accordance with the experience.

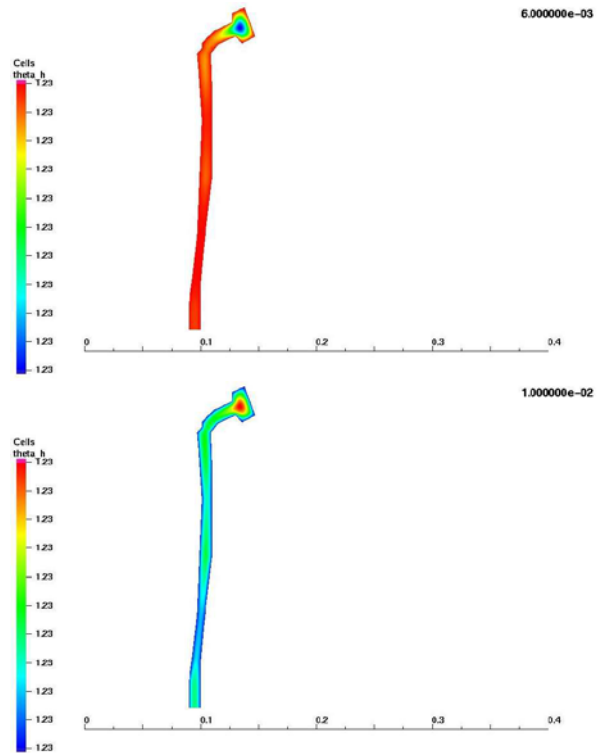


Figure 5: Temperature distribution at two different instants of the rubber bladder curing process. An inversion of the hot and cold zones may be observed.

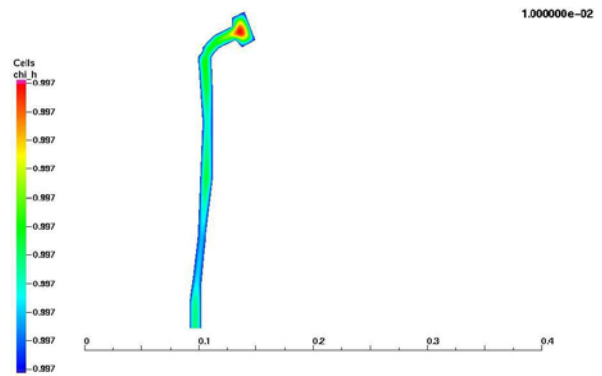


Figure 6: Reactant's concentration in the rubber bladder curing process simulation.

### CONCLUSIONS

A model based on the balance of internal heat generation due to reaction and heat transfer through the mold walls is presented and analyzed. A finite element implementation of the model was done with the ALBERTA Finite Element Toolbox. This implementation was used to simulate an experimental testing device and the obtained results were confronted with experimental data, showing a good performance. A two dimensional problem was then simulated to test the implementation and finally, the

model was applied to the simulation of the curing process of a rubber bladder as those employed in tire manufacturing, with an actual bladder geometry.

## REFERENCES

- Andre, M. and M. Wriggers. 2005. "Thermomechanical behavior of rubber materials during vulcanization". *International Journal of Solids & Structures*, No.42, 4458-4478.
- ASTM F433-02 "Standard practice for evaluating thermal conductivity of gasket materials". ASTM International, PA.
- Broyer, E. and C. Macoskos. 1976. "Heat transfer and curing in polymer reaction molding". *AIChE Journal* 22, No.2, (Mar), 268-276.
- Ghoreishy, M.H.R. and G. Naderi 2005. "Three-dimensional finite element modeling of rubber curing process". *Journal of Elastomers and plastics*, No. 37, 37-53.
- In-Su Han *et al.* 1999. "Optimal curing steps for product quality in a tire curing process". *Journal of Applied Polymer Science*, 74, 2063-2071.
- Juma, M. and M. Bafnec. 2004. "Experimental determination of rubber curing reaction heat using the transient heat conduction equation". *Chemical Papers* 58, No.1, 29-32.

- Mark, J., B. Erman, and F. Eirich. 2005. *The science and technology of rubber*. 3rd. Edition. Elsevier Academic Press, Amsterdam.
- Schmidt, A. and K. G. Siebert. 2005. *Design of adaptive finite element software. The finite element toolbox ALBERTA. LNCSE 42*. Springer, Berlin.

## AUTHOR BIOGRAPHIES

**DANIEL KOESTER** was born in Kiel, Germany. He studied Mathematics and Physics at the Universities of Kiel and Freiburg. He obtained his diploma in August, 2003. He is currently employed at the University of Augsburg and completing his Ph. D. thesis on the simulation and modelling of microfluidics. His e-mail address is: koester@math.uni-augsburg.de

**PAULO PORTA** was born in Rosario, Argentina. He studied Engineering and obtained his degree in 1992. He worked at Universidad Tecnológica Nacional, Argentina and at the University of Augsburg, Germany, where he got his Ph.D. Currently he is a senior researcher at DARMEX S.A.C.I.F.I., Argentina. His e-mail address is : pporta@darmex-int.com